Influence of Melonic acid on the Corrosion Inhibition of Sodium Metavanadate in Chloride Medium

Sribharathy V.[1*] and Susai Rajendran[1, 2]
[1]Corrosion Research Centre, Department of Chemistry, GTN Arts College, Dindigul-624005, Tamil Nadu, INDIA
[2]Department of Chemistry, RVS School of Engineering and Technology, Dindugul-624005, Tamil Nadu, INDIA

Abstract

The inhibition efficiency (SMV) – melonic acid system is controlling corrosion of carbon steel in an aqueous solution containing 60 ppm of Cl- has been evaluated by weight loss method.250 ppm of SMV has 56% of IE. Addition of melonic acid to SMV improves the inhibition efficiency of the system. Formulation consisting of 250 ppm of SMV and 250 ppm of melonic acid has 96% IE. Synergistic effects exist between SMV and melonic acid, if the synergism parameters are greater than 1. Mechanistic aspects of corrosion inhibition have been studied by electro chemical studies like polarization and electro chemical impedance spectroscopy. FTIR spectra reveals that the protective film consists of Fe2+ - SMV complex and Fe2+ - melonic acid complex, the protective film has been analyzed by fluorescence spectra, SEM and AFM .

Keywords: Carbon steel, corrosion inhibition, fluorescence, synergism parameter, SEM.

Introduction

Vanadium –based oxyanions, also referred to as vanadate, have been investigated as corrosion inhibitors for Al alloy. However they have not gained much attention probably due to the relatively large solubility of vanadium oxides in aqueous solution[1-4]. Smith et al explored the release kinetics and protection performance of vanadate –based pigment in epoxy coated MA2014-T6 panel. A later investigation by cook et al screened and compared several inhibitors including vanadates, molybdates, and ion of rare earth elements like Ce, Y, and La[5]. The author analyzed the behaviour of aqueous solutions containing vanadium oxoanions and concluded that metavanadate, ie., vanadate oligomers including V1, V2, V4 and V5 co-ordination are not potent inhibitors of oxygen reduction reaction (ORR) but significantly lower the anodic dissolution kinetics[6]. Recently chamber et al studied the synergism of several binary and ternary mixture including vanadate, phosphate, molybdate and rare earth elements. The author concluded that the maximum synergistic effect occurred for vanadate-phosphate solution in ratio 50:50[7].

The co-ordination chemistry of vanadium oxoanions in aqueous solutions is rather complex. It involves several protonation/deprotonation reactions, as well as polymerization to form oligomers of varied depending upon pH and concentration[8-12].

pH values between 6 and 9 leads to formation of colourless (or) yellow metavanadate [V3O93-] [13-16] this suggest that vanadates are inhibitors of corrosion, and it seems likely the inhibition depends on speciation.

The objective of this work: Clear metavanadate solutions containing monovanadate exhibited strong inhibition of the oxygen reduction reaction, to a level similar to chromate. At a fixed pH, increased NaVO3 concentration in clear metavanadate solution increased inhibition efficiency.

Material and Methods

Preparation of extract: Sodium metavanadate was prepared by dissolving 1g of SMV in double distilled water and making up to 100 ml. This solution was used as a corrosion inhibitor in the present study.

Preparation of Specimens: Carbon steel specimens (0.0267% S, 0.06% P, 0.4% Mn, 0.1% C and the rest iron) of dimensions 1.0 cm x 4.0 cm x 0.2 cm were polished to a mirror finish and degreased with trichloroethylene.

Weight loss Method: Carbon steel specimens in triplicate were immersed in 100 ml of the solutions containing various concentrations of the inhibitor (sodium metavanadate and melonic acid solution) for three day. The weight of the specimens before and after immersion were determined using Shimadzu balance, model AY 62. The corrosion products were cleansed with Clarke's solution[16]. The inhibition efficiency (I.E.) was then calculated using the equation

$$IE = 100 \left[1-(W2/W1)\right] \% \tag{1}$$

Where W1 = Corrosion rate in the absence of the inhibitor, W2 = Corrosion rate in the presence of the inhibitor

Surface Examination: The carbon steel specimens were immersed in various test solutions for a period of one day, taken

out and dried. The nature of the film formed on the surface of metal specimens was analyzed by FTIR spectroscopic study.

FTIR Spectra: FTIR spectra were recorded in a Perkin – Elmer 1600 spectrophotometer. The film was carefully removed, mixed thoroughly with KBr made in to pellets and FTIR spectra were recorded.

Scanning Electron Microscopic studies: The carbon steel immersed in blank and in the inhibitor solution for a period of one day was removed, rinsed with double distilled water, dried and observed in a scanning electron microscope to examine the surface morphology measurements of the carbon steel were examined using JOEL 6390 model computer controlled scanning electron microscope.

Atomic Force Microscopy characterization (AFM): The carbon steel immersed in blank and in the inhibitor solution for a period of one day was removed, rinsed with double distilled water, dried and subjected to the surface examination. The surface morphology measurements of the mild steel surface were carried out by atomic force microscopy (AFM) using veeco innova.

Potentiodynamic Polarization: Polarization studies were carried out in an H and CH Electrochemical Work station Impedance Analyzer Model CHI 660A. A three electrode cell assembly was used. The working electrode was carbon steel. A saturated calomel electrode (SCE) was used as the reference electrode and a rectangular platinum foil was used as the counter electrode.

AC Impedance Measurements: The instrument used for polarization was used for AC impedance study also. The cell set up was the same as that used for polarization measurements. The real part and imaginary part of the cell impedance were measured in ohms at various frequencies. The values of charge transfer resistance, Rct, and the double layer capacitance, Cdl were calculated.

Synergism parameter (S_I): Synergism parameter is indication of synergistic effect existing between the inhibitors[17] value is found to be greater than 1 suggesting that the synergistic effect between the inhibitors.

$$S_I = \frac{I - I_{1+2}}{I - I'_{1+2}} \qquad (2)$$

I_1 = Surface coverage ($\theta 1$) of inhibitor SMV, I_2 = Surface coverage of inhibitor ($\theta 2$) Melonic acid, I'_{1+2} = Combined surface coverage of inhibitor SMV and MA

Analysis of Variance: F-test was carried out to investigate whether synergistic effect existing between inhibitor system is stastically significant[18]. If F-value is above 5.32 for 1,8 degree of freedom, it was proved to be stastically significant. If the value is below 5.32 for 1, 8 degree of freedom, it was stastically insignificant at 0.05 level of significance confirmed.

Results and Discussion

Weight loss study: Evaluation of improvement of IE smv with melonic acid: The inhibition efficiency (IE) of sodium metavanadate (smv) in controlling the corrosion of carbon steel immersed in aqueous solution containing 60 ppm of Cl^- for a period of three days is given in table 1. It is seen from the data that SMV alone shows some IE; where as melonic acid shows some IE. When SMV is combined with melonic acid ions. For example 250ppm of SMV has only 56% and 250ppm of melonic acid has 85% IE interestingly their combination shows 96% IE This suggests a synergistic effect existing between the binary inhibitor formulation SMV and melonic acid ions.

Synernism parameter: The value of synergism parameters are shown in table 2. The value of S_I is greater than one, suggesting synergistic effect. SI approaches 1 when no interaction exists between the inhibitor compounds. When SI>1, this points to synergistic effect. In the case of SI<1, the negative interaction of inhibitor prevails (i.e., corrosion rate increases).

Analysis of variance (ANOVA): F-test is used if the synergistic effect exist between inhibitors is statistically significant. The results are given in table 3. Influence of various concentration of melonic acid (50,100,150, 200 and 250ppm) on the Inhibition efficiency of SMV (250ppm) is shown in the table 3. The calculated F-value is 14.8. It is statistically significant, since it is greater than the critical value (5.32) for 1, 8 degree of freedom of 0.05 level of significance. Hence it is concluded that the influence of 250ppm of SMV to the various concentration of melonic acid shows statistically significant.

Effect of Sodiumdodecylsulphate (SDS) on the inhibition efficiency of SMV-MA system: The influence of various concentration of SDS on the IE of the SMV-MA system is shown in table 4. It is observed that the IE of SMV-MA with 150ppm of SDS system was 98%. It is interesting to note that the sodium metavanadate - MA system has some biocidal efficiency (BE) in table 5. The BE increases from 67 to 98. When 150ppm of SDS is added 250ppm, 100% BE is noted. The formulation consisting of 250ppm of SMV, 250ppm of MA and 150 ppm of SDS has 100% BE and 98% of corrosion inhibition efficiency. This formulation may find application, if the investigation is carried out at high temperature and under flow condition.

FTIR spectra: The FTIR spectrum of pure SMV is shown in Fig 1a VO_3^- stretching frequency appears at 1385 $cm^{-1.}$ The FTIR spectrum of pure melonic acid is shown in Fig 1b. The -C=O stretching frequency appeared at 1719 cm^{-1}. –OH stretching frequency appeared at 3407 cm^{-1}. –CH_2 stretching frequency appeared at 2976 cm^{-1}. The FTIR spectrum (KBr pellet) of the film formed on the carbon steel surface after

immersion in the solution containing 250ppm of SMV, 250ppm of melonic acid as shown in figure 1c. The VO_3^- stretching frequency of SMV shifted from 1385 cm^{-1} to 1386 cm^{-1} resulting in the formation of Fe^{2+} -SMV complex. The –C=O stretching frequency shifted from 1719cm^{-1} to 1638 cm^{-1} and -

OH stretching frequency shifted from 3407cm^{-1} to 3439cm^{-1}. This suggest that oxygen atom of melonic acid co-coordinated with Fe^{2+} on the anodic sides of the metal surface, resulting in the formation of Fe^{2+}- MA complex[19-20].

Table-1
Corossion rates (CR) and Inhibition efficiencies (IE) of carbon steel in aqueous solution containing 60 ppm of Cl⁻ in the absence and the presence of Inhibitors and Inhibition efficiency (IE) obtained by weight loss method

Smv ppm	Melonic Acid ppm	IE%	CR(mdd)
0	0	-	22.73
50	0	8	20.91
100	0	12	20.10
150	0	29	15.19
200	0	32	12.50
250	0	56	10.00
0	50	62	8.637
0	100	65	7.955
0	150	78	5.000
0	200	83	3.8641
0	250	85	3.4095
250	50	90	2.27
250	100	92	1.818
250	150	94	1.3638
250	200	95	1.3665
250	250	96	0.9092

Table-2
Synergism parameters of carbon steel immersed in in aqueous solution containing 60 ppm of Cl⁻ in the absence and the presence of Inhibitor

MA ppm	IE%	θ_2	SMV ppm	IE%	θ_1	IE%	θ'_{1+2}	S_I
50	62	0.63	250	56	0.56	90	0.90	1.6
100	65	0.65	250	56	0.56	92	0.92	1.9
150	78	0.78	250	56	0.56	94	0.94	1.6
200	83	0.83	250	56	0.56	95	0.95	1.4
250	85	0.85	250	56	0.56	96	0.96	1.6

Table-3
Distribution of F value between the inhibition efficiencies of smv –MA system

Source of variance	Sum of square	Degree of freedom	Mean square	F	Level of significance
Between	1708	1	1708	14.8	$p > 0.05$
With in	479	8	115		

Table-5
Corrosion rate carbon steel in aqueous solution containing 60 ppm of Cl⁻ in presence and absence of inhibitors and the corrosion inhibition efficiencies by the weight loss method

SMV ppm	MA ppm	SDS ppm	CR	IE %	Colony forming units ml	Biocidal efficiency
0	0	0	-	-	1×10^5	-
0	0	150	-	-	2.5×10^4	84
250	250	50		67	1.9×10^4	89
250	250	100	4.77	78	1.5×10^3	92
250	250	150	0.68	98	1.1×10^3	94
250	250	200	0.68	98	4×10^2	97
250	250	250	0.68	98	nil	100
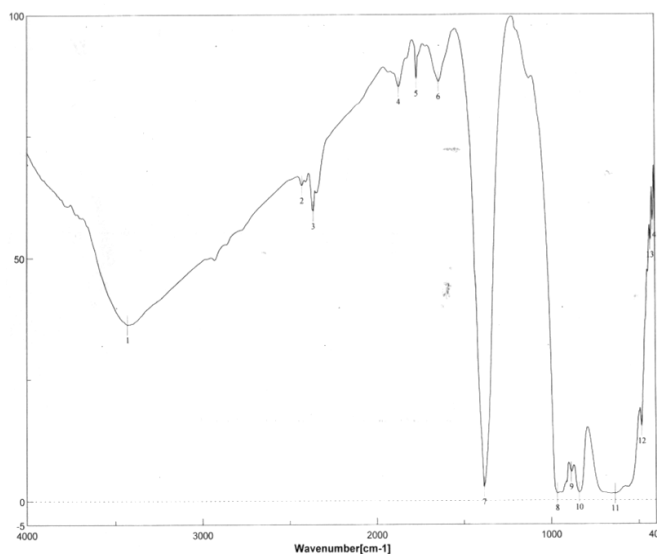
Figure-1(a)
Pure SMV
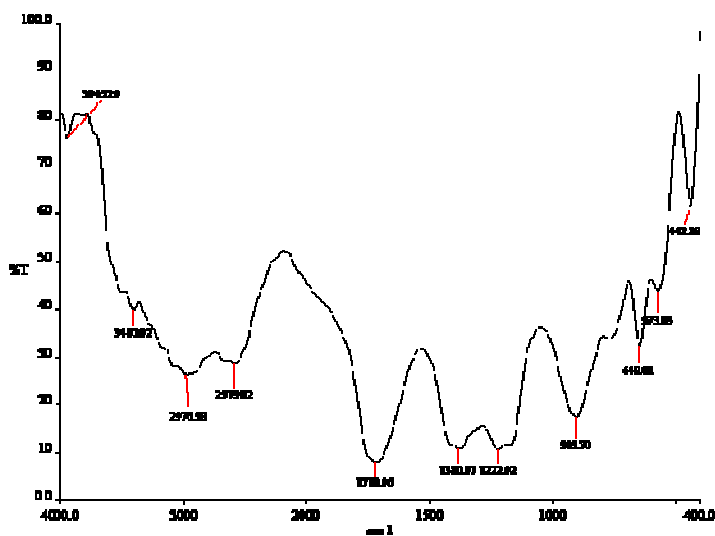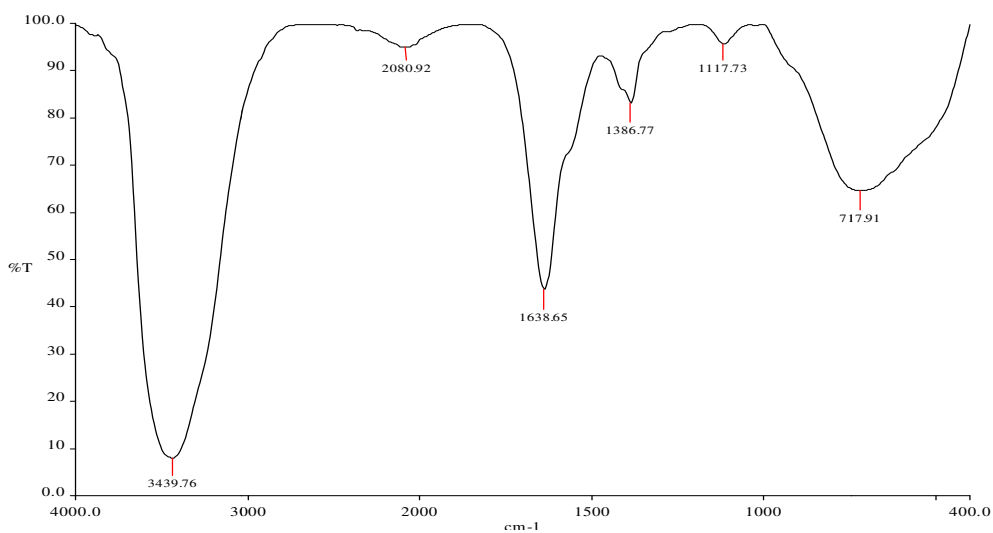
Figure-1(b)
Pure melonic acid

Figure-1(c)
Film formed on surface of metal after immersion in aqueous solution containing 60 ppm of Cl⁻

Analysis of Polarization Study: The potentiodynamic polarization curves of metal immersed in aqueous solution containing 60 ppm of Cl⁻ figure 2. The corrosion potential (Ecorr), Tafel slope (bc= cathodic; ba= anodic, linear polarization resistance LPR and corrosion current Icorr are given in table 6.

The potentiodynamic polarization curves of carbon steel immersed in aqueous solution containing 60 ppm of Cl⁻ are shown in figure 2. The corrosion parameters are given in table 6.

When carbon steel is immersed in aqueous solution containing 60 ppm of Cl⁻ the corrosion potential Ecorr -542mV vs SCE. When 250ppm of SMV and 250ppm of melonic acid are added to the above system, the corrosion potential Ecorr-599 mV vs SCE shifted to the cathodic side. The cathodic Tafel slope (bc) is 193 and anodic Tafel slope (ba) is 198 mV/ Decade. It is inferred that the change of current with change in potential is less during cathodic polarization than during anodic polarization[21-22].

The LPR values is 2.0157×10^{4} Ωcm^2 and the corrosion current is 2.025×10^{-6} A/cm2 When carbon steel is immersed in aqueous solution containing 60 ppm of Cl- (figure 2). The corrosion potential is shifted to cathodic side -599 mV vs SCE. This suggests that a protective film is formed on the metal. The cathodic and anodic Tafel slopes were shows difference 72 mV /decade this shows change of current with change in potential is less during anodic polarization than during cathodic polarization.

The LPR value increase from 2.0157×10^{4} to 3.4693×10^{4} Ωcm^2. The corrosion current decrease 2.025×10^{-6} to 1.270×10^{-6} .An increase in LPR value and decrease in corrosion current are indicating ions protective film on the metal surface[23].

The polarization curves in the solution with no inhibitor were identical except for a change in the open current potential (OCP). All polarization curves in the metavanadate- containing solutions exhibited much lower OPR rates, and there was no influence of pH. This suggest that the local cathodes are blocked by V1 which greatly reduces the rate of oxygen reduction, since monovanadate appears to be the strongest corrosion inhibitor of the system, any coating scheme based on vanadium should release V1. This suggests that cathodic inhibition by vanadate is largely through the suppression of oxygen reduction with little effect on hydrogen evolution.

AC Impedance spectra: AC impedance spectra of metals immersed in aqueous solution containing 60 ppm of Cl- are shown in figure 2. Nyquist plot and bode plots are shown in (figure 3 and 4). The charge transfer resistance (Rct) and double layer capacitance (C_{dl}) values (derived from Nyquist plots) and impedance , $\log(Z/\Omega)$ value derived from bode plots are given in table 7. When mild steel is immersed in aqueous solution

containing 60 ppm of Cl⁻ the charge transfer resistance is 2363 Ω cm^2 and the double layer capacitance is 2.1919×10^{-9} F/cm2 (figure 4). The impedance log (Z/ Ω), value 3.237

When carbon steel immersed in aqueous solution containing 60ppm of Cl⁻ the charge transfer resistances increases from 2363 to 3679 Ω cm^2 and the double layer capacitance value decreases from 2.1919×10^{-9} to 1.38×10^{-10} F/cm^2. The impedance value increases from 3.237 to 3.55. This indicates the film formed on the metal surface[24-25].

SEM Analysis of Metal surface: The SEM image of magnification (x 500) of carbon steel specimen immersed in aqueous solution containing 60 ppm of Cl⁻ for 1 day in the absence and presence of inhibitor system are shown in figure 5 (a,b,c).

The SEM micrographs of polished carbon steel surface (control) in figure 5 (a) shows the smooth surface of the metal this shows the absence and presence of any corrosion products formed on the metal surface[26].

The SEM micrographs of carbon steel surface immersed in aqueous solution containing 60 ppm of Cl⁻ in figure 5 (b) shows the roughness of the metal surface which indicates the corrosion of carbon steel in aqueous solution containing 60 ppm of Cl⁻. figure 5 (c) indicates the presence of 250 ppm SMV and 250 ppm melonic acid, the surface coverage increases which in turn results in the formation of insoluble complex on the surface of the metal and the surface is covered by a thin layer of inhibitors effectively control the dissolution of carbon steel.

Atomic Force Microscopy: Atomic force microscopy is a powerful technique for the gathering of roughness statistics from a variety of surfaces[27-29]. AFM is becoming an accepted method of roughness investigation.

Atomic force microscopy provided direct insight in to the changes in the surface morphology take place at several hundred nanometers when topological changes owing to the initiation of corrosion and formation of protective film on the metal surface in presence and absence of inhibitors respectively.

All atomic force microscopy images were obtained on vecco innova instrument operating in tapping mode in air. The scan size of all the AFM images are 5µm x 5 µm areas at a scan rate of 6.4 lines per second.

The two-dimensional (2D) and three-dimensional (3D) AFM morphologies and the AFM cross-sectional profile for polished carbon steel surface (reference sample), carbon steel surface immersed in aqueous solution containing 60 ppm of Cl- (blank sample) and aqueous solution containing 60 ppm of Cl- 250 ppm of SMV and 250 ppm melonic acid are shown in figure 6 (a,b,c), (d,e,f) respectively.

Root mean square Roughness, average roughness and maximum peak to valley Height: AFM image analysis was performed to obtain the average roughness, Ra (the average deviation of all points roughness profile from a mean line over the evaluation length), root –mean – square roughness, Rq (the average of the measured height deviations taken within the evaluation length and measured from the mean line) and the maximum peak to valley (P-V) height values (largest single peak-to-valley height in five adjoining sampling heights). Rq is much more sensitive than Ra to large and small height deviations from the mean.

The value of Rq, Ra and P-V height for the polished carbon steel surface (reference sample) are 3.41nm, 4.33 nm and 43.5 nm respectively. This shows a more homogenous surface, with some places in where the height is lower than the average depth. Figure 6 (a) displays the un-corroded metal surface. The slight roughness observed on the polished metal surface is due to atmospheric corrosion. The rms roughness, average roughness and P-V height values for the carbon steel surface immersed in aqueous solution containing 60 ppm of Cl⁻ are 21.2662 nm,

17.2138 nm and 63.5 nm respectively. The data suggest that the carbon steel surface immersed in aqueous solution containing 60 ppm of Cl⁻ has a greater surface roughness than the polished metal surface, which shows that the unprotected carbon steel surface is rougher and were due to the corrosion of carbon steel in aqueous solution containing 60 ppm of Cl⁻ environment. Figure 6 (b) displays corroded metal surface with few pits.

The formulation consisting of 250 ppm SMV and 250 ppm melonic acid in aqueous solution containing 60 ppm of Cl⁻ reduces the Rq value of 4.1nm and the average roughness is significantly reduced to 2.4 nm when compared with 34 nm for carbon steel surface immersed in aqueous solution containing 60 ppm of Cl⁻. The maximum peak to valley height was also reduced to 34 nm. These parameters confirm that the surface appears smoother. The smoothness of the surface is due to the formation of a protective film of Fe^{2+}- SMV complex and Fe^{2+}-MA complex on the metal surface thereby inhibiting the corrosion of carbon steel which confirms the formation of the film on the metal surface, which is protective in nature.

Table-6
Corrosion parameter of carbon steel immersed in aqueous solution containing 60 ppm of Cl⁻ obtained by polarization study are given

System	Ecorr (mV vs SCE)	bc (mvVs /decade)	ba (mv /decade)	LPR Ω cm^2	Icorr (A/ cm^2)
Aqueous solution containing 60 ppm of Cl⁻	- 542	193	198	2.0157 x 104	2.025 x10-6
Aqueous solution containing 60 ppm of Cl⁻ + 250 ppm SMV+250 ppm MA	-599	162	270	3.4693 x 104	1.270x 10-6

Table-7
Impendence parameter of carbon steel immersed in aqueous solution containing 60 ppm of Cl⁻ in the presence and absence of inhibitor system obtained from AC impedance curves

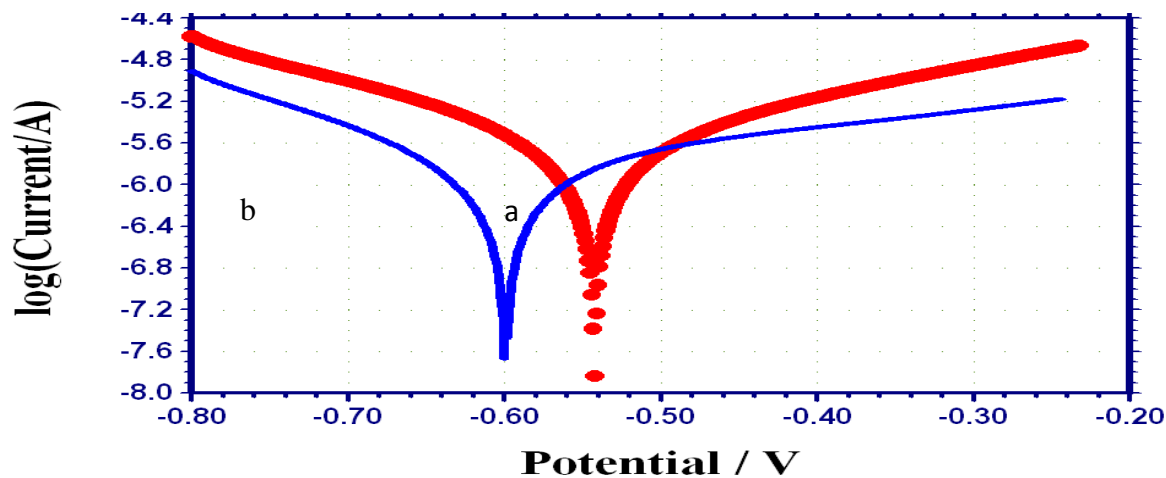| system	Nyquist plot		Bode plot
	Rct Ωcm2	Cdl F/cm2	Impedance log(Z/Ω)
Aqueous solution containing 60 ppm of Cl⁻	2363	2.1919x10^{-9}	3.237
Aqueous solution containing 60 ppm of Cl⁻ + 250 ppm SMV+250 ppm MA	4264	1..19x 10^{-9}	3.55

Figure-2
Polarization curves of carbon steel immersed in various test solutions, (a) Aqueous solution containing 60ppm of Cl⁻
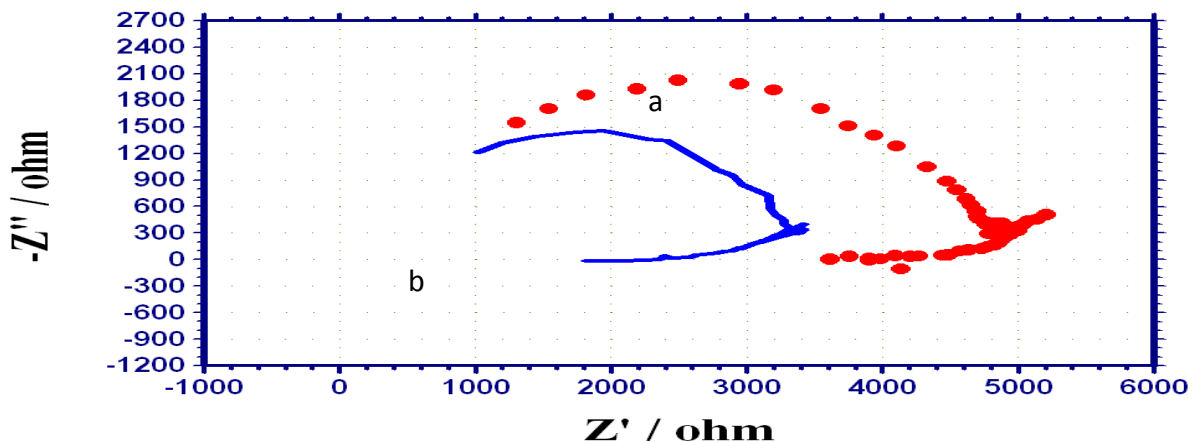**(b) Aqueous solution containing 60ppm of Cl⁻+250 ppm SMV+ 250 ppm MA**

Figure-3
AC Impedance spectra of carbon steel immersed in various test solution, (a) Aqueous solution containing 60ppm of Cl⁻, (b)
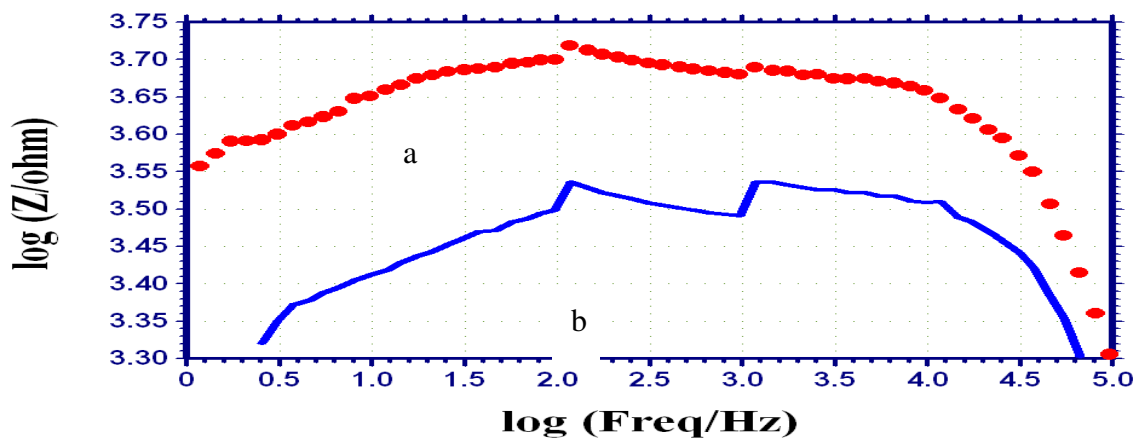**Cl⁻ 60ppm (Nyquist)   Cl⁻ 60ppm+ 250ppm SMV+250ppm MA (Nyquist)**

Figure-4
AC Impedance spectra of carbon steel immersed in various test solution, (a) Cl⁻ 60ppm (impedance-bode), (b) Cl⁻ 60ppm +
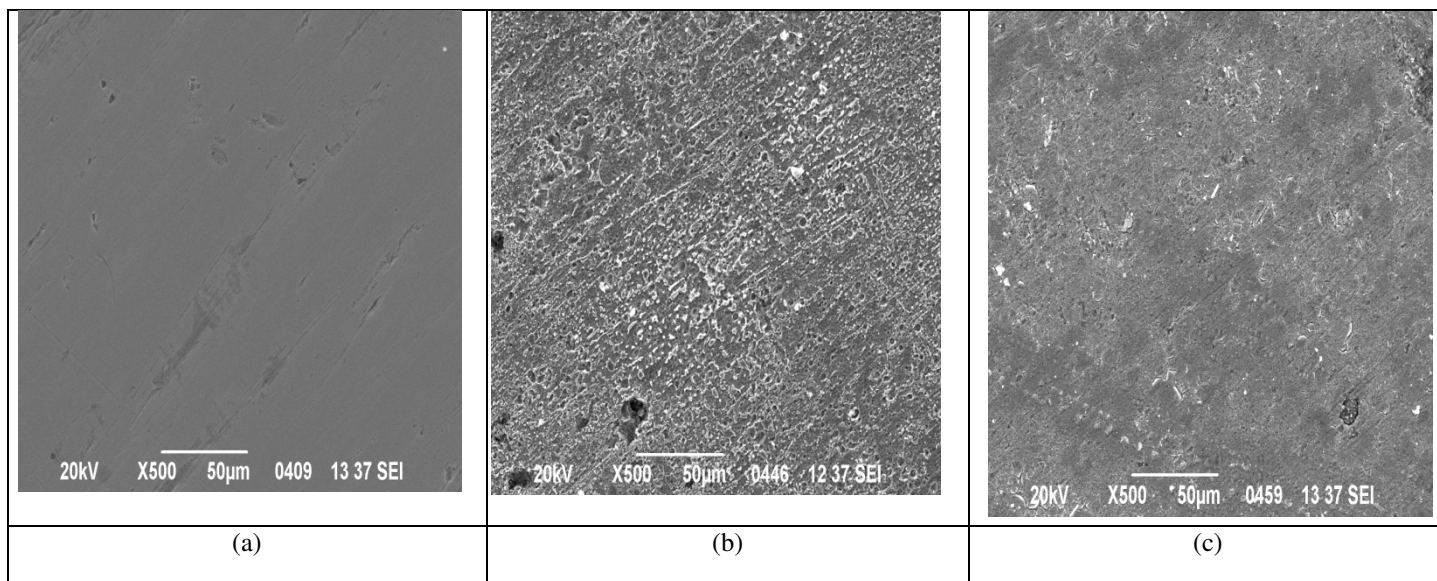**250ppm SMV+250ppm MA (impedance-bode)**

| (a) | (b) | (c) |

Figure-5
SEM micrographs of (a) Polished carbon steel (control); Magnification –X 500. (b) Carbon steel immersed in aqueous solution containing 60 ppm of Cl⁻; Magnification –X 500. (c) Carbon steel immersed in aqueous solution containing 60 ppm of Cl⁻ + 250 ppm of SMV+ 250 ppm of MA; Magnification –X 500

Table-8
Summary of the average roughness (Ra), rms roughness (Rq), maximum peak –to-valley height (P_V) value for carbon steel surface immersed in different environments

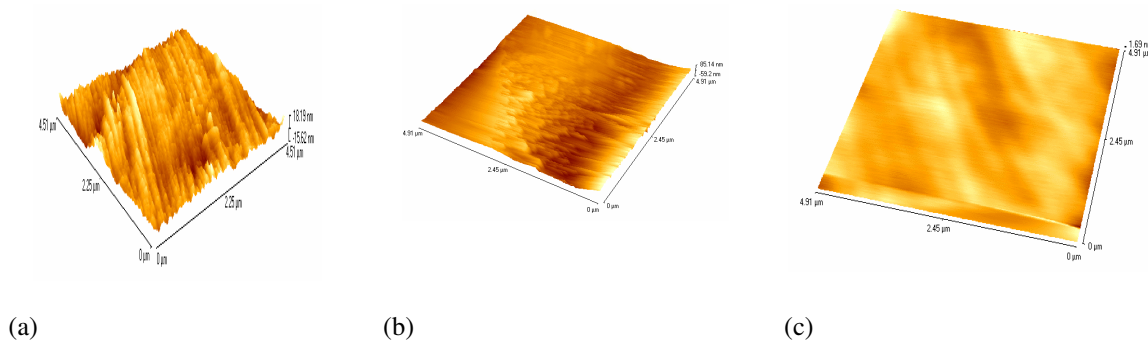| Samples	RMS(Rq) Roughness(nm)	Average(Ra) Roughness(nm)	Maximum peak-to-valley height(nm)
Polished carbon steel(control)	4.33	3.41	43.5
60 ppm of Cl⁻	17.2138	21.2662	63.5
60 ppm of Cl⁻+SMV(250 ppm) + MA(250 ppm)	4.1	2.4	34

| (a) | (b) | (c) |

Figure-6
AFM image of the surface of a) polished carbon steel (control), carbon steel immersed in aqueous solution containing 60 ppm of Cl⁻, carbon steel immersed in aqueous solution containing 60 ppm of Cl⁻+ 250 ppm of SMV+ 250 ppm of MA

(d)   (e)   (f)

Figure-6

Cross sectional profile, which are corresponding to as shown broken lines AFM image of the surface of polished carbon steel (control) carbon steel immersed in aqueous solution containing 60 ppm of Cl⁻ carbon steel immersed in aqueous solution containing 60 ppm of Cl⁻+ 250 ppm of SMV+ 250 ppm of MA
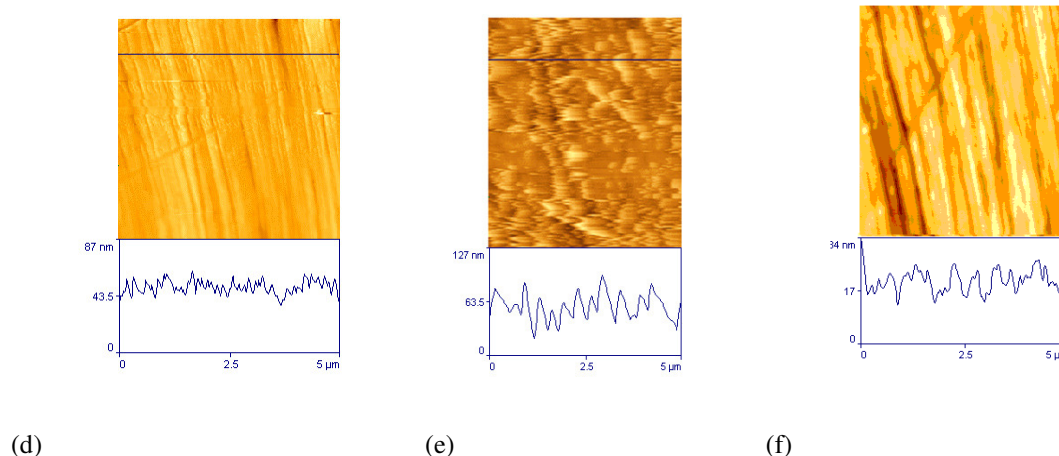
Conclusion

The present study leads to the following conclusion: The formulation consisting of 250 ppm of MA and 250 ppm of SMV offers 98% inhibition efficiency to carbon steel immersed in aqueous solution containing 60 ppm Cl⁻. Polarization study reveals that this formulation controls anodic reaction predominantly. AC impedance spectra reveal that a protective film formed on the metal surface. FTIR spectra and also reveal that the protective film consists of Fe^{2+}-SMV complex and Fe^{2+}-MA complex. SEM and AFM study confirm that protective film formed on the metal surface

Acknowledgement

References

1. Kending M. and Buchheit R.G., Corrosion Inhibition of Aluminium and Aluminium Alloys by Soluble Chromates, Chromate Coatings and Chromate-Free Coatings Corrosion (Houston), **59(5),** 379-400 **(2003)**

2. Iannuzzi M., Young T. and Frankel G.S, Aluminum Alloy Corrosion Inhibition by Vanadates *J. Electrochem. Soc.,* **153(12),** B533-B541 **(2006)**

3. Guan Hand Buchheit R.G, Corrosion (Houston), **60,** 284-294 **(2004)**

4. Ralston K.D., Chrisanti S., Young T.L. and Buchheit R.G., Corrosion Inhibition of Aluminum Alloy 2024-T3 by Aqueous Vanadium Species, *J. Electrochem. Soc.*, **155(7),** C350-C359 **(2008)**

5. Cook R.L. and T. aylor S.R., Characterization of Inhibitor Release from Zn-Al- [V10O28] 6–Hydrotalcite Pigments and Corrosion Protection from Hydrotalcite- Pigmented Epoxy Coatings Corrosion (Houston), **56**, 321-333**(2000)**

6. Buchheit R.G., Guan H., Mahajanam S., and Wong F., Active corrosion protection and corrosion sensing in chromate-free organic coatings, *Prog. Org. Coat.*, **47(9)**174-182 **(2003)**

7. Chambers B.D., Taylor S.R., and Kending M.W., Corrosion (Houston), **51**, 480-489 **(2005)**

8. Crans D.C. and Tracey A.S., Peroxo-, Hydroxylamido- and acac-derived Vanadium Complexes, *ACS Symp. Ser.*, **7(11)**, 2-29 **(1998)**

9. Petterson L. and Elvigson K., *ACS Symp, Ser.*, **7(11),** 30 **(1998)**

10. Petterson L., Equilibria of polyoxometalates in aqueous solution, *Mol. Eng.*, **3(1-3)**, 29-42 **(1993)**

11. Cruywagen J.J., Mo (VI) and W(VI) removal from water samples by acid-treated high area carbon cloth, *Adv. Inorg. Chem.*, **49** 127-182 **(2000)**

12. Holleman A.F. and Wiberg E., Inorganic chemistry, Academic Press, New York **(2011)**

13. Frankel G.S. and. Mc Creery R.L, Releasable corrosion inhibitor compositions, Interface, (USA) 34-38 **(2001)**

14. Campestrini P., Goeminne G., Terryn H. and Vereecken J., Corrosion Resistance of Cr (III)Based Conversion Layer on Zinc Coatingsin Comparison with a raditional Cr (VI)Based Passivation Treatment, *J. Electrochem. Soc.*, **151**, B59- B70 **(2004)**

15. Crompton J.S, Andrews P.R. and Alpine E.M, Characteristics of a conversion coating on aluminium Surf., *Interface Anal.*, **13,** 160 **(1988)**

16. Wranglen G., Introduction to corrosion and protection of metals, London: chapman and Hall 236 **(1985)**

17. Rajendran S., Vaibhavi S. and Anthony N., Inhibitive action of hydroquinone - Zn^{2+} system in controlling the corrosion of carbon steel in well watercorrosion, **59,** 529-534 **(2003)**

18. Rajendran S., Raji A., Arokiaselvi A., Rosaly J. and Thangaswamy, Parents' education and achievement scores in chem- istry Edutracks, **6,** 30-34 **(2007)**

19. Agnesia Kanimozhi S. and Rajendran S., Inhibitive Properties of Sodium tungstate-Zn2+ System and its Synergism with HEDP, *International J. Electro Chem Sci.,* **4**, 353-368 **(2009)**

20. Silver stein R.M, Bassler G.C and. Morrill T.C., Spectroscopic Identification of organic compound, Newyork, NY: John Wiley and sons, 95 **(1986)**

21. Sathyabama J., Susai R. Arokia S.J. and John A.A, Methyl orange as corrosion inhibitor for carbon steel in well water Indian, *J chem Tech*, **15,** 462-466 **(2008)**

22. Rajendran S., Sridevi S.P., Anthony N., John Amalraj A. and Sundaravadivelu N., Corrosion behaviour of carbon steel in polyvinyl alcohol, *Anti Corro. Methods Maerial*, **52,** 102-107 **(2005)**

23. Felicia Rajammal Selvarani, Santhanalakshmi S., Wilson Sahayaraja J., John Amalraj A. and Susai Rajendran, Corrosion inhibition of carbon steel by succinic acid – Zn2+ system, *Bull.Electrochemistry*, **20,** 561-565 **(2004)**

24. Sathiyabama J., Susai Rajendran, Arokia selvi J., Bull. Electrochemistry, Methyl orange as corrosion inhibitor for carbon steel in well water, **22,** 363-370 **(2006)**

25. Susai Rajendran, Manimaran M., Wilson Sahayaraja J., Sathiyabama J., John Amalraj A. and Palaniswamy N., Trans., SASET, **41,** 462-466 **(2006)**

26. Rajendran S., Manimaran M., Investigation of inhibitive action of urea- zn2+ system in the corrosion control of carbon steel in sea water, International Journal of Engineering Science and Technology (IJEST), **3(11)**, 8048-8060 **(2011)**

27. Dumas Ph., Butffakhreddine B., Am C. OVatel E., Ands, Galindo R. and Salvan F., Quantitative Microroughness Analysis down to the Nanometer Scale Europhys, Lett, **22,** 717-722 **(1993)**

28. Bennet J.M, Jahannir J., Podlesny J.C, Baiter T. Land Hobbs D.T, Analysis of nano film by atomic force microscopy Appl, Opt, **43,** 213-230 **(1995)**

29. Amra C., Deumie C., Torricini D., Roche P., Galindo R., Dumas P. and Salvan F., Combination of surface characterization techniques for investigating optical thin-film components Int, Symp. on Optical Inference coating, SPIE 2253 614-630 **(1994)**